PURPOSE-LED PUBLISHING™

PAPER • OPEN ACCESS

Comparison of classical and drone based hard-target methodologies applied to scanning lidar for offshore wind

To cite this article: A Oldroyd *et al* 2024 *J. Phys.: Conf. Ser.* **2875** 012041

View the article online for updates and enhancements.

Comparison of classical and drone based hard-target methodologies applied to scanning lidar for offshore wind

**A Oldroyd[1*], M Young[1], M Docherty[1],
J Bost[2], S Redford[2], J Haize[2], J Royle[3],
J Gottschall[4]**

[1] Oldbaum Services Limited, Stirling, UK
[2] TotalEnergies, Aberdeen, UK
[3] K2M, Glasgow, UK
[4] Fraunhofer Institute for Wind Energy Systems IWES, Bremerhaven, Germany

[*]E-mail: andy@oldbaum.co.uk

Abstract. Hard target testing is a crucial part of the commissioning process of scanning lidar measurement systems. The correct alignment of the scan head and understanding of the pointing accuracy is crucial to reducing uncertainties in wind speed measurements by scanning lidar especially in dual-scanning configuration. This paper presents a comparison between traditional hard targeting technique and the use of drone based hard targets. A procedure is presented to minimise measurement error and hence increase confidence in the pointing accuracy.

1   Introduction

The study reported here is part of the West of Orkney Windfarm (WoOW) project which is a 2.25 GW offshore wind farm project, situated off Scotland`s north coast. The project is located approx. 23 km from the Caithness coast, Scotland, and 28 km from the west coast of Hoy, Orkney. Metocean climates are expected to be harsher than those experienced on other UK offshore wind farms in terms of wind conditions. To study these conditions in more detail a comprehensive measurement campaign has been commissioned.

As part of the measurement campaign, two long range Vaisala Windcube 400S scanning lidar (SL) systems have been deployed on the archipelago of Orkney – see Figure 1.

In recent years, DSL has become a powerful wind measurement tool capable of providing high quality data and serving several use-cases. However, the systems are very sensitive to setup and require a thorough understanding of their measurement capability using campaign settings (via verification) and detailed calibration of the scan head position at each install [3, 4]. Recent work within the framework of the Offshore Wind Accelerator (OWA) Global Blockage Effect in Offshore Wind (GloBE) project [5] have further emphasized the importance in determining the offsets, as part of the scan head calibration, when applying scanning lidar to different use-cases and the implications of improper setup in achieving the goals of a measurement campaign which has been here the experimental identification of the Global Blockage Effect (GBE). Scan head calibration is normally carried out during the system installation and commissioning stage. The calibration process involves the identification and mapping of hard targets, understanding their true location and calculating offsets defined as the difference between the true target location and the target location as observed by the scanning lidar. Often hard targets used in an offshore environment are turbines or transitions pieces (TPs). In [6] it was proposed to use the sea surface

instead, which however requires that the SL has a good all-round view not being significantly restricted by the installation setup. Ships and drones are suggested as possible alternatives in [7].
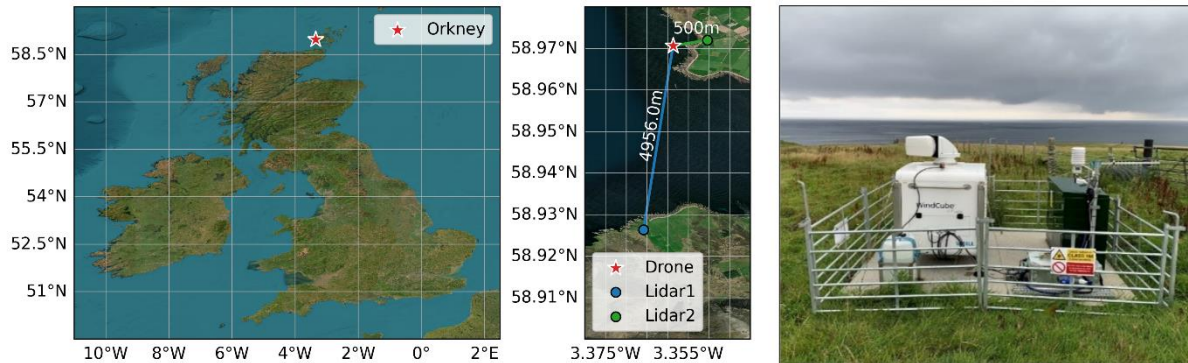

Figure 1: Left shows the location of DSL wind measurements used for the West of Orkney Windfarm project; middle shows overview map of the drone hard target test setup with the two SL "Lidar1" and "Lidar2"; right side Southern SL (Lidar1) of type Vaisala Windcube 400S.

Within this contribution we further investigate the use of drones as a possible solution for hard-target tests (HTTs) when installations occur in locations with no, few, or not suitable (fixed) hard targets. While drones have an obvious potential for HTTs and have drawn more attention recently (being not just mentioned in [7] but also discussed in ongoing IEC 61400-50-5 [8] work), there are few reported cases of their use for HTTs and few instances where systematic procedures have been implemented to determine suitable drone HTT methods and the positional accuracy associated with these.

In this contribution, we introduce a systematic process for using drones in SL scan head position calibration whereby the accuracy of the drone HTT method is assessed and compared to the traditional hard target method. We look at two drone targeting approaches, being beam acquisition (BA) and drone acquisition (DA), respectively. Drone acquisition is where the drone is flown to an expected beam location based on install geometry and calibration, and beam acquisition is the process of acquiring the drone hard target, where the drone position is known to a high degree of confidence.

With the findings from our study we intend to answer the following questions: how can hard target testing using drones be best implemented, what are the associated uncertainties and how can these be minimized. Following this brief introduction we outline the applied methodology in section 2; results of the study are described in section 3 with details about the run tests, specific findings for the two drone targeting approaches and the uncertainty assessment. A short discussion of the above specified questions and the final conclusions follow in section 4 and 5, respectively.

2 Methodology

The method of hard target adjustment is described in detail in [2] whereby it is differentiated between cases with (at least) three hard targets allowing for a sine curve fit to the errors, and cases with fewer hard targets. Figure 2 (left) shows an example of lidar elevation angle errors derived from two HTTs which were executed for the same SL device; one test using three hard targets was conducted by the OEM prior to installation, and the second test used only one hard target as part of the setup for performance verification (PV) by a verification consultant. For both cases, an elevation error is derived as the difference between the SL elevation angle setting and a

reference reading, displayed as function of the SL azimuth angle. The typical sine curve is a result of both internal (mechanical alignment) and external (pitch and roll) SL characteristics. For the initial example in Figure 2 (left) we observe on the one hand a perfect sine curve for the HTT by the OEM but on the other hand a substantial deviation for the HTT during PV, giving rise to speculations about the accuracy and repeatability of both tests.
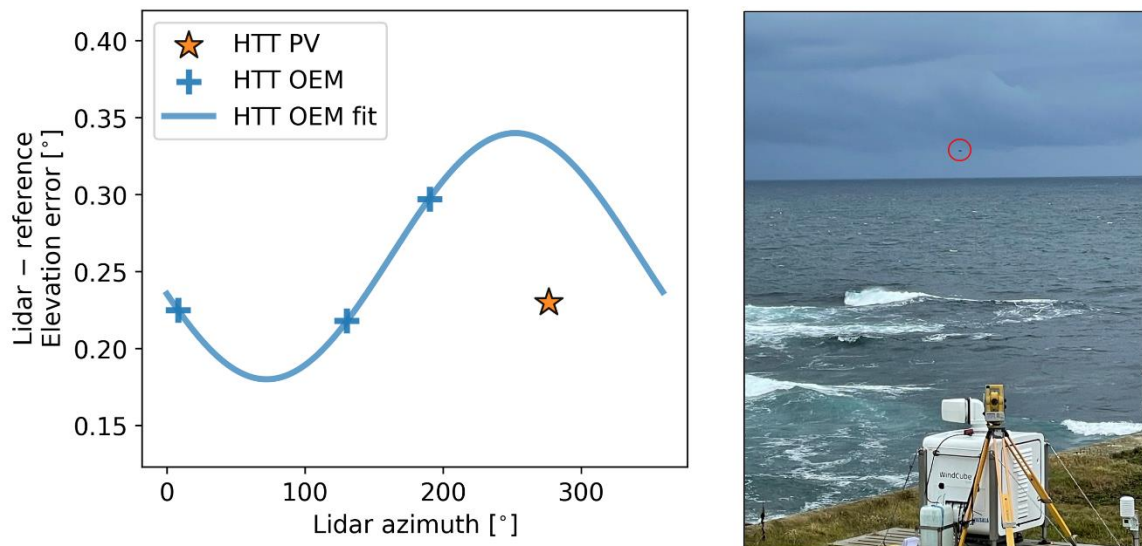

Figure 2: (Left) Lidar elevation angle errors and resulting sine curve fit as a function of lidar azimuth derived from hard target testing (HTT) with results provided by the lidar OEM, and a third party for the unit performance verification (PV) test; (right) Northern SL WC400S with reference theodolite in foreground; the drone target is marked with a circle in the photo.

Besides further investigating the deviation shown in Figure 2 (left), the purpose of the drone-based HTT was to determine the impact of distance on the scan head position assessment. To do this we have defined two testing methods:

- <u>Method 1 – Drone Acquisition (DA)</u>: The beam position co-ordinates and elevation <u>are</u> calculated at specified ranges from the SL. The drone is flown to that position and the SL Carrier-to-Noise Ratio (CNR) response is checked. If there is no CNR spike (to indicate drone acquisition), the scanner head is moved until the drone is acquired. The GPS location and height of the drone are recorded.
- <u>Method 2 –Beam Acquisition (BA)</u>: The drone is flown to a fixed position. The SL is operated and the CNR map is examined to acquire the drone. Once a position is defined, the elevation and azimuth angle of the drone target is recorded.

For each considered measurement location, an azimuth and elevation angle relative to the SL location was determined, and it was planned to use both acquisition methods to assess which approach is most effective. Figure 2 (right) shows the Northern SL with the target drone in the distance located 500 m from shore at a prescribed height (c.f. Figure 1; middle). The height was chosen based on the expected measurement campaign elevation angle to represent a project relevant measurement height at a range of 7 km from shore.

The drone used as the hard target was a MatriceRTK350 drone linked to a GPS base station to improve positional accuracy. A reference theodolite base station was installed and operated by a trained Chartered Surveyor at the Northern SL location as is shown in Figure 2 (right). With this setup and according to system specifications a vertical accuracy of 1.5 cm can be reached. Non-

optimal environmental conditions, particularly high winds as discussed in the next section, resulted in higher uncertainties.

3 Results

The drone-based HTTs took place over two days on the 4th and 5th October 2023 with the results detailed in the following subsections. In 3.1, we show the trial results and compare them with standard HTTs performed for the same SL device. In 3.2, we further elaborate on the two introduction acquisition methods, and 3.3 summarises the uncertainty assessment for both standard (based on fixed hard targets) and drone-based HTTs.

3.1 Hard target testing results

The onsite weather conditions in Orkney were not ideal in the available test window. The drone system recorded wind speeds in excess of 16m/s consistently throughout Day 1. Day 2 was a little calmer at 9 m/s. Completion of the measurement programme was possible with certain limitations (mainly available flight time).

Before we focus on the drone HTT results, we review two tests with fixed hard targets which were conducted at an earlier stage of the measurement campaign (Figure 3).
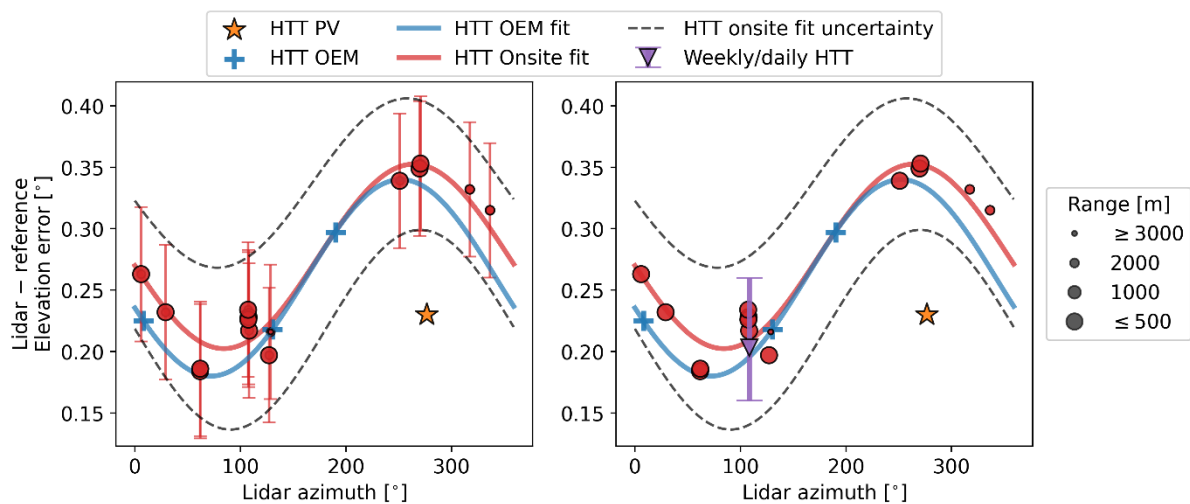

Figure 3: Lidar elevation angle errors and resulting sine curve fits as a function of lidar azimuth derived from hard target testing (HTT) – as in Figure 2 (right). Left panel includes elevation errors derived from hard target testing during site installation; right hand side additionally shows regular (weekly/daily) fixed hard target test results derived during a long-term period. Further details in main text.

Figure 3 (left) is an extension of Figure 2 (left), including elevation errors derived from onsite HTTs during site installation, with target acquisition range delineated by marker size. The error bars represent the total test uncertainties derived from adding the lidar and theodolite elevation uncertainty components, as further discussed in 3.3, together in quadrature. The dashed grey lines are the uncertainty in the sine curve fit derived from the onsite HTT results. The stacked points around 100 degrees lidar azimuth are a result of picking hard targets that are too close together - in this case a row of fence posts in a field. The close azimuthal proximity of the posts plus errors associated with selecting the correct hard target pixels from CNR mapping result in an ambiguous result.

Figure 3 (right) additionally includes regular (weekly/daily) fixed HTT results derived during a long-term period (162 tests during a 7-month period), with the purple marker depicting the mean error, and purple error bar representing the full range (minimum to maximum) of

elevation errors observed during the period. The results are compared with the installation setup and expected results, showing a close agreement to the sine curve fits from both the OEM and site installation tests, and with error bars within the range of expected uncertainty. This gives confidence in the repeatability of the process and continued scan head control of the WC 400S during the campaign.

The results of the drone-based HTT are finally included in Figure 4. The green markers show the elevation angle errors derived from the drone HTT, with error bars representing the total uncertainty in the elevation error based on estimates of the lidar and theodolite uncertainty components but not yet the drone movement uncertainty – again, see 3.3 for a discussion of the uncertainty components.
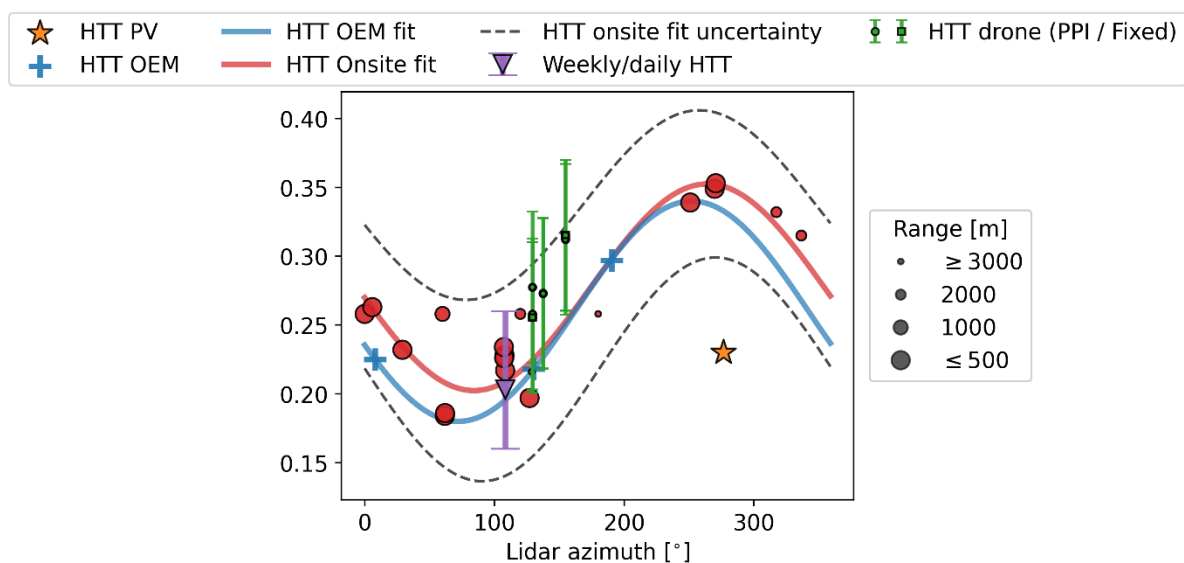

Figure 4: As Figure 3 but also including elevation angle uncertainties derived from drone hard target testing – further details in main text.

The drone HTT results are within the uncertainties of the standard (fixed HTT) results but with a slightly higher error which might be due to some likely further alignment requirement in the different geometry reference systems used in calculating relative positions as well as because of the adverse weather conditions and drone stability during our tests. In addition, the entire sine curve cannot be reproduced, which is due to the fact that the planned test programme could not be completed (again due to adverse weather conditions).

3.2 Beam acquisition versus drone acquisition

The Matrice RTK350 drone type has been chosen as it has a high predicted position stability. However, in our case due to the weather it was clear the drone was having some problems in maintaining position. Figure 5 shows a timeseries of CNR observed from a fixed line-of-site measurement during the drone test. A signal with CNR >-7dB at a measurement range of approximately 4.9 km corresponds to acquisition of the drone hard target. Here the drone is stable for a period before it drifts out of the lidar line-of-site.
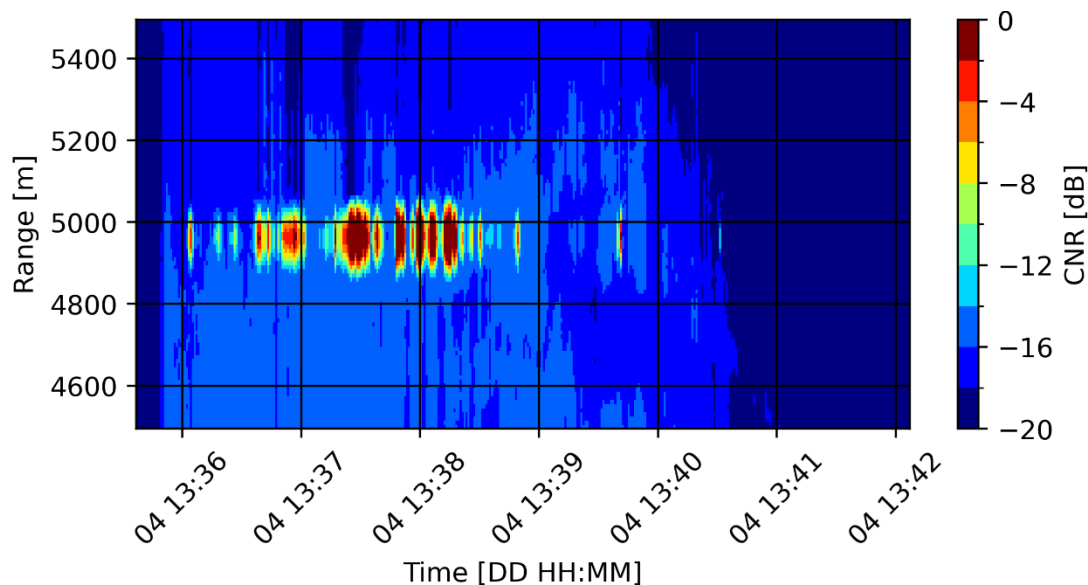
Figure 5: Example time series showing CNR [dB] as a function of measurement acquisition range [m] and time during a fixed line-of-site measurement with beam azimuth of 4.59° and elevation of 0.95°.

Due to that drift, the DA method was not possible to achieve. BA however was successfully achieved on all flights despite very short flight times with less than 15 minutes in the target location on Day 1. In better conditions on Day 2, a more stable, hybrid, procedure was followed, consisting of the following steps:

- Step 1: calculate the expected geometries and fly drone to target location;
- Step 2: set SL to acquire drone and conduct a narrow angle, high resolution beam search for the drone (BA);
- Step 3: once the drone is acquired, reset the SL and re-programme in the expected drone location (DA).

With this method the drone was acquired quickly with the chosen hard target azimuth and elevation angle verified during step 3. These are the results presented previously in Figure 4.

3.3 Uncertainty estimation
Table 1 presents a first approximation of the uncertainty quantification comparing the drone and traditional HTT methods. The individual components are further explained in the following.

Table 1: HTT uncertainty components – SL and the theodolite uncertainties are added in quadrature to estimate the total uncertainty for the hard target test (cf. Figures 3 and 4). The drone and curve fit uncertainties are kept separate as these are additional uncertainty components that are test specific.

Source	Uncertainty	Definition	Value
SL	$\Delta_{SL\text{-}pos}$	scan head movement (pitch/roll)	$\pm 0.02°$
	$\Delta_{SL\text{-}ext}$	drone extent from CNR mapping	$\pm 0.05°$
Theodolite	$\Delta_{Ref\text{-}acc}$	instrument accuracy	$\pm 0.0014°$
	$\Delta_{Ref\text{-}pos}$	uncertainty due to scan head – theodolite height difference	$\pm 0.01°$
Total (SL + Theod.)	Δ_{HTT}	$(\Delta_{SL\text{-}pos}{}^2 + \Delta_{SL\text{-}ext}{}^2 + \Delta_{Ref\text{-}acc}{}^2 + \Delta_{Ref\text{-}pos}{}^2)^{1/2}$	$\pm 0.055°$

Drone	$\Delta_{\text{HT-pos}}$	drone positional uncertainty	test specific
Curve fit	Δ_{CF}	curve fit on points	test specific

From the lidar there are two main contributing factors: the size of the hard target, picking the correct azimuth and elevation from the detailed CNR map, and system movement (particularly the scan head) during beam acquisition. An example of scan head movement is shown in Figure 6 displaying pitch and roll data from the SL during the test period. Here it is possible to see a shift in mean pitch as the scan head was prepared for the BA process. The shaded areas represent the extent of the lidar system pitch and roll movement, and once the scan head is moved there is little variation in values during the periods when the hard target process took place (grey shaded areas). The variation in pitch and roll may be concerning, however this is when the scanner moves at maximum rate. The movement is seen even though the scanning lidar is secured to a solid stable base.
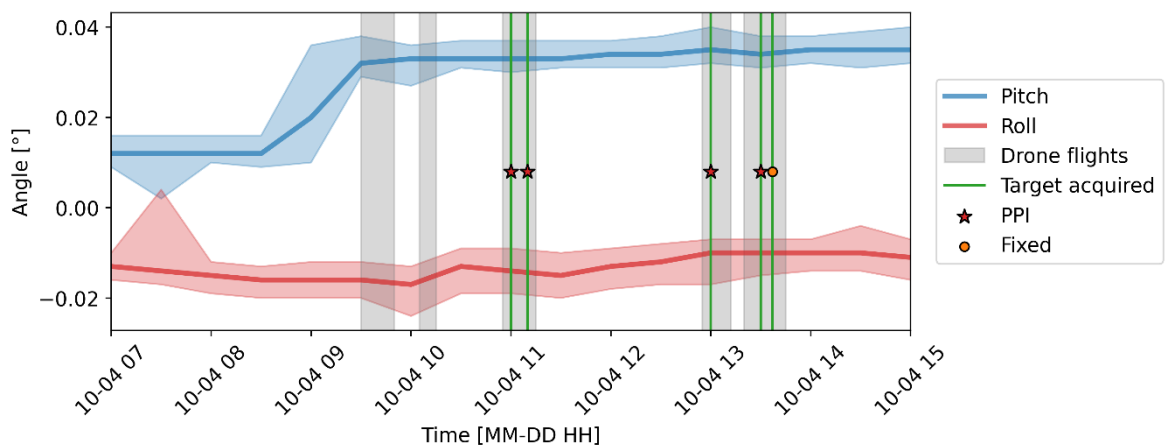

Figure 6: Timeseries of lidar system half-hourly pitch and roll (mean – lines; range – shading) during the drone hard targeting test period.

Figure 7 shows two CNR maps measured during drone acquisition at roughly 5 km and 500 m distance, respectively. For both cases it becomes clear that picking the drone centre corresponding to the drone GPS position can be subject to error. This mapping uncertainty ($\Delta_{\text{SL-ext}}$) does not only occur for drone-based HTTs but also for the more standard fixed hard targets with values estimated to be in a similar range as the 0.05° in Table 1. This order of magnitude also corroborates with results reported from the standard fixed target method in [3].
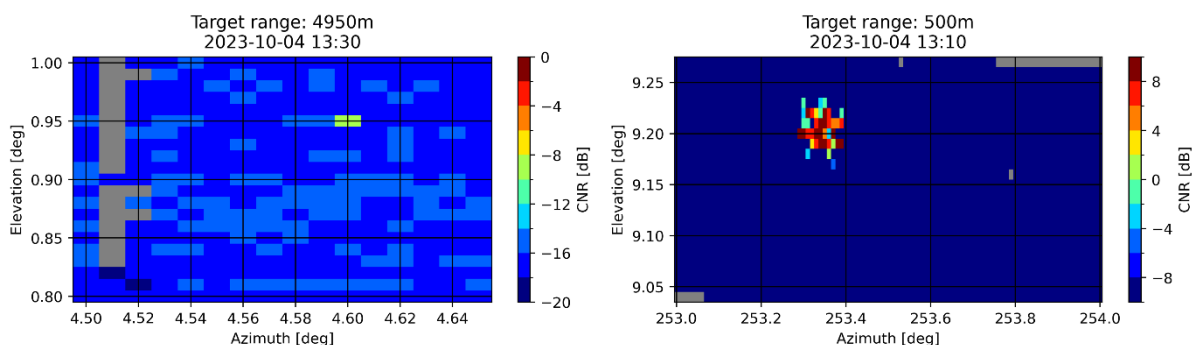

Figure 7: CNR measurements as a function of azimuth and elevation angle during drone acquisition at 5 km range (left) and 500 m range (right).

The reference theodolite uncertainty in Table 1 is based on best practice guidance and the precision of the instrument once calibrated using standard references as conducted by the Chartered Surveyor.

The drone positional uncertainty can be very test specific, and has been in our case strongly influenced by the prevailing high wind conditions which were, as discussed before, not optimal. Assuming a ± 1.5m height variation in a drone flight at 500 m range may correspond to an elevation angle variation of ±0.17°, which is by far much higher than all other uncertainty components.

4   Discussion

Drone-based HTT has been suggested as a solution to offshore scan head alignment. While there is obvious potential for the technique, in practice there are a number of challenges that need to be addressed before a robust procedure can be presented to the wind community. As illustration of this, compare the left and right-hand sides of Figure 7. The left-hand side is the drone representation at 5 km. The right-hand side is the drone at 500 m. The drone is much clearer at 500 m, but the error associated with establishing the centre of the drone is conversely higher.

As described in 3.3, the results of the drone-based HTT must be assigned a considerable higher uncertainty in comparison to the standard (fixed) HTT results, with the drone positional uncertainty being by far the highest contribution. We believe this component can be significantly reduced in more favourable prevailing environmental conditions (e.g. lower wind speeds) and by following an optimized process covering the three steps listed in 3.2. Errors can be further reduced by iterating the two actions of (1) identifying the target from a detailed CNR map, and (2) plotting the scan head sine curve using targets at different azimuths and estimating the error offset from this.

Using the outlined procedure, we believe at a minimum, a similar level of uncertainty can be achieved as with the traditional method, making it applicable for fully offshore scan head alignment. However, this has yet to be confirmed in further test campaigns. But even if these levels cannot be reached, drone-based HTTs can be useful either to confirm previous tests (as in this paper) or in a setup where no other hard targets can be used for assessing the scan head alignment and positional accuracy of a SL measurement.

5   Conclusion

The potential of drone-based scan head calibration has been considered obvious particularly in absence of fixed hard targets typically used for this exercise, however there are several factors that require better definition before a clear testing procedure is available to the wind community. This paper highlights some of the areas of concern with respect to test conditions and error associated with attributing the correct hard target reference to the offset calculations. Based on our experience we have suggested an updated procedure to establish the correct offsets using drone hard targeting. The work will continue examining in more detail the uncertainty quantification and looking further into the optimisation process to automate the procedure.

Acknowledgements

References

[1]   NEDO 2023 Offshore Wind Measurement Guidebook (March 2023),
        https://www.nedo.go.jp/content/100962731.pdf (last accessed 28-07-2024)

[2]   DNV and Vaisala 2024 Guidelines on dual scanning lidar measurements for wind resource assessments,
        Tech. Report Rev. 0 (5 March 2024), https://www.vaisala.com/sites/default/files/documents/WEA-ERG-
        Whitepaper-Guidelines-dual-scanning-lidar-measurements-WRA.pdf#page=25&zoom=100,76,436 (last
        accessed 28-07-2024)

[3]   N Vasiljevic, G. Lea, M Courtney, J-P Cariou, J Mann and T Mikkelsen, 2016, Remote Sens. 8(11),
        896; https://doi.org/10.3390/rs8110896

[4]   S Shimada, J Prakash Goit, T Ohsawa, T Kogaki and S Nakamura 2020 Remote Sens. 12, 1347;
        doi:10.3390/rs12081347

[5]   N. Adams, C. Rodaway, J. Gottschall, G. Hawkes, E. Simon, WESC 2023 Mini-Symposium – OWA GloBE:
        Building Industry Consensus on the Global Blockage Effect in Offshore Wind,
        https://zenodo.org/doi/10.5281/zenodo.8085204

[6]   A Rott, J Schneemann, F Theuer, J J Trujillo, and M Kühn 2022 Wind Energ. Sci., 7, 283–297,
        https://doi.org/10.5194/wes-7-283-2022

[7]   Carbon Trust 2023 OWA Scanning LiDAR Best Practice for Power Curve Testing,
        https://www.carbontrust.com/our-work-and-impact/guides-reports-and-tools/guidelines-for-scanning-
        lidars-for-power-curve-testing (last accessed 28-07-2024)

[8]   International Electrotechnical Commission IEC 61400-50-5: Use of scanning doppler lidars for wind
        measurements, Technical Specification under development (status 2024)